Supporting Information for *Acta Phys. -Chim. Sin.* 2016, *32* (9), 2318－2326
doi: 10.3866/PKU.WHXB201605181

超分子聚合物刷 PVP-Chol 表面图案化及其力诱导的可逆结构转变

刘姗姗　　季　姗　　陈启斌*　　彭昌军　　刘洪来

(华东理工大学化学系，化学工程国家重点实验室，上海 200237)

Surface Patterning and Force-Induced Reversible Structural Transformation of a PVP-Chol Supramolecular Polymer Brush

LIU Shan-Shan　　JI Shan　　CHEN Qi-Bin*　　PENG Chang-Jun　　LIU Hong-Lai

(*State Key Laboratory of Chemical Engineering, Department of Chemistry, East China University of Science and Technology, Shanghai 200237, P. R. China*)

*Corresponding author. Email: qibinchen@ecust.edu.cn; Tel: +86-21-62252921.

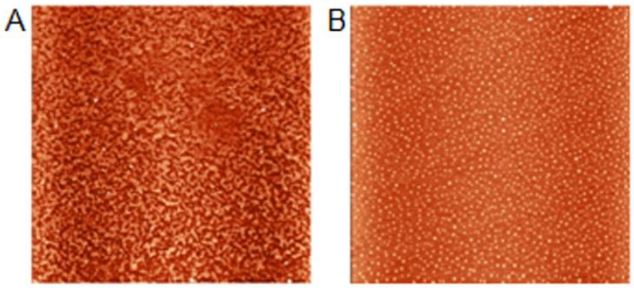

Fig.S1 AFM height images of the spin-coating film of PVP-Chol complex at 5.0 × 10^{-4} mol Ł$^{-1}$ in $CHCl_3$

(A) random coil structure; (B) spherical particle. The sizes of A and B are 10 μm × 10 μm.

In Fig.S1, the morphology of stoicghiometric PVP-Chol complex in $CHCl_3$ presented two structures: one is the random coil structure, the number of such aggregates is ~30% on the basis of an evaluation of more than 30 independent AFM images with a scanning size of 10 μm × 10 μm; and the other is the spherical particle, the number is ~70%. The original structure of supramolecular polymer brush PVP-Chol can not obtain by spin-coating method.

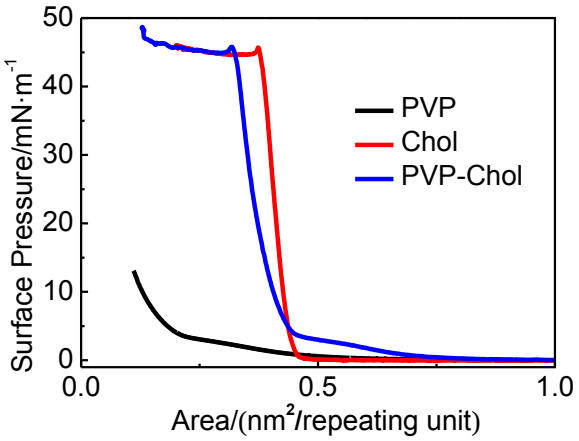

Fig.S2 *π*–*A* isotherms of PVP, Chol, and PVP-Chol complex at 5.0 × 10^{-4} mol Ł$^{-1}$ with the subphase temperature of 20 °C

The molecular area of PVP-Chol is based only on the molecular weight of cholesterol.

In Fig.S2, the limiting area of PVP-Chol, by extrapolating the steepest portion of the *π*-*A* curves to $\pi = 0$, is ~0.41 nm^2, close to the area of pure cholesterol (0.44 nm^2), illustrating that the majority of PVP macromolecules enters into the subphase during

increasing the operating pressure, and only a small quantity of PVP-Chol reserves and maybe continue to assemble with cholesterol molecules at the higher surface pressures.

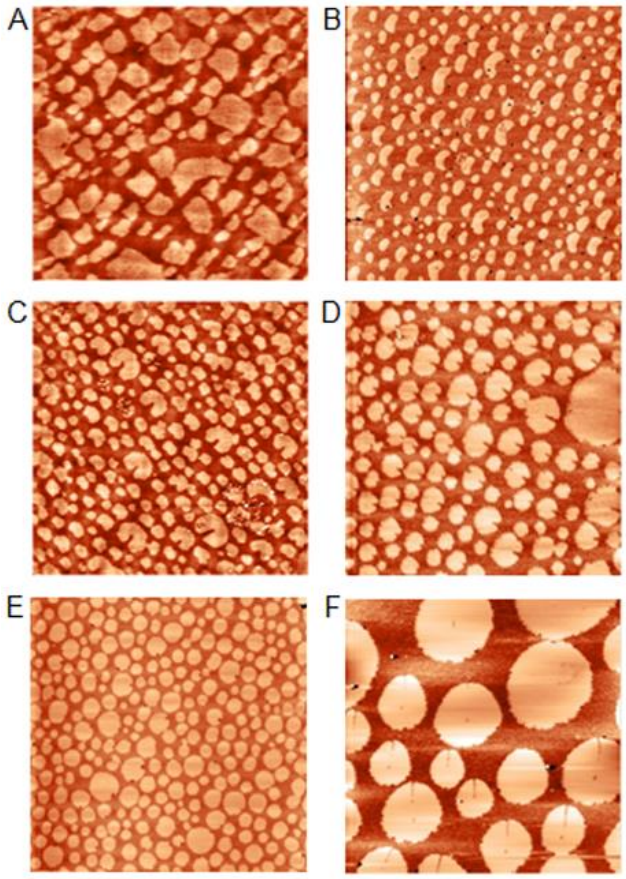

Fig.S3 Morphology of phase separation of PVP-Chol complex at the lower surface pressures of (A) 0, (B) 0.2, (C) 0.5, (D) 0.7, (E) 1 and (F) 2 mN m^{-1}

A, C and E are height images, while the others are phase images. The sizes of all images are 30 μm × 30 μm.

In Fig.S3, with the surface pressure increasing, the brighter domains become more ordered, from the initially irregular shape at 0 mN m^{-1} (Fig.S3A) to crescent shape at 0.2 mN m^{-1} (panel B), then heart-shaped (panel C, 0.5 mN m^{-1}; panel D, 0.7 mN m^{-1}) and circular (panel E, 1.0 mN m^{-1}) configuration. Subsequently, the circular domains become larger at 2.0 mN m^{-1} (panel F). This indicates that such surface patterning is tightly connected with the surface pressure at the air/water interface.

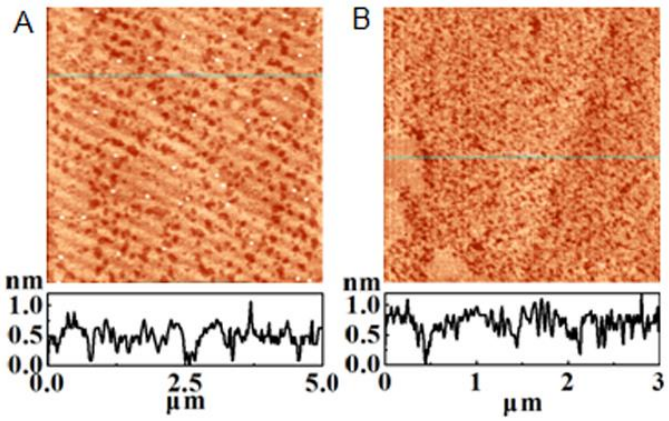

Fig.S4 AFM images of pure PVP at low surface pressures of (A) 0, (B) 2.0 mN ṁ$^{-1}$

The AFM height images of PVP monolayer at low surface pressures show dense and random fibrous structure.

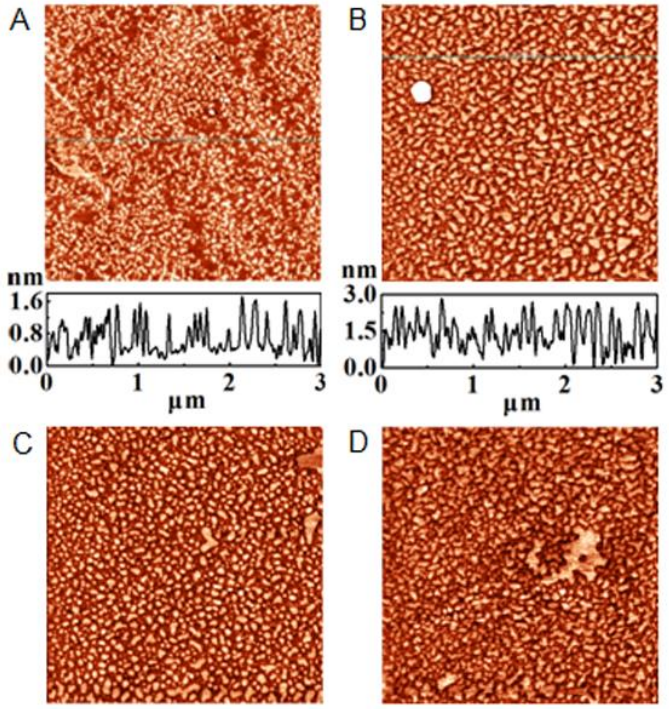

Fig.S5 AFM height images of pure cholesterol at different surface pressures of (A) 0, (B) 1.0, (C) 5.0 and (D) 10.0 mN ṁ$^{-1}$

The sizes of all images are 3 μm × 3 μm.

The surface topographies of cholesterol monolayer show a negligible change after the 1.0 mN ṁ$^{-1}$ with the dynamic compression of barriers.

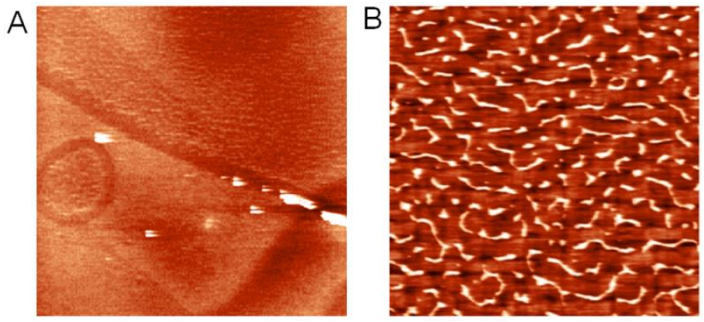

Fig.S6 AFM height images of PVP-Chol at 5.0 mN m^{-1}

The sizes of A and B are 20 μm × 20 μm and 3 μm × 3 μm, respectively.

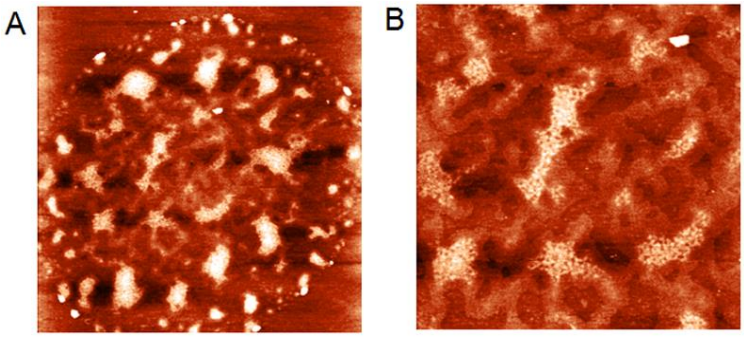

Fig.S7 AFM height images of PVP-Chol at 2.5 mN m^{-1}

The sizes of A and B are 10 μm × 10 μm and 5 μm × 5 μm, respectively.

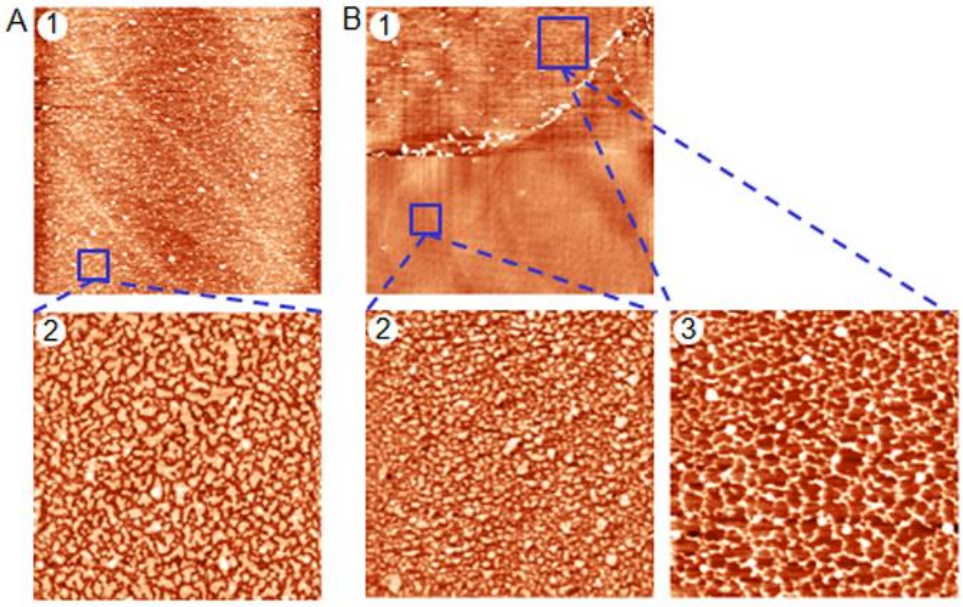

Fig.S8 AFM height images of PVP-Chol complex at 10.0 mN m^{-1}

(A), the representative and amorphous structure of pure cholesterol in most areas of LB films (ca. 90%). Panel 2 (3 μm × 3 μm) is the zoomed in image of panel 1 (30 μm × 30 μm). (B), the coexistence of two different structures: one is the dominant structure of cholesterol (panel 2, 3 μm × 3 μm), the other is fibrous aggregates of PVP-Chol (panel 3, 3 μm × 3 μm) which accounts for ~10% of the whole area of LB films. Panels 2 and 3 are the amplified images of panel 1 (30 μm ×

30 μm).

In Fig.S8, the morphology of PVP-Chol complex at 10.0 mN m^{-1} shows the coexistence of two different structures. One is the featureless structure accounts for a substantial part of region, i.e., approximate 90%, according to the evaluation of more than 20 independent AFM images with a scanning size of 30 μm × 30 μm. Here, the whole topography of the three AFM images is this structure in four images (scanning size: 30 μm × 30 μm), as shown in Fig.S8A. Such featureless structure is identical to that of cholesterol at high surface pressures (Fig.S4). The other is fibrous aggregates of PVP-Chol which accounts for ~10% of the whole area of LB films in more than 20 independent AFM images (panel 3 of Fig.S8B).

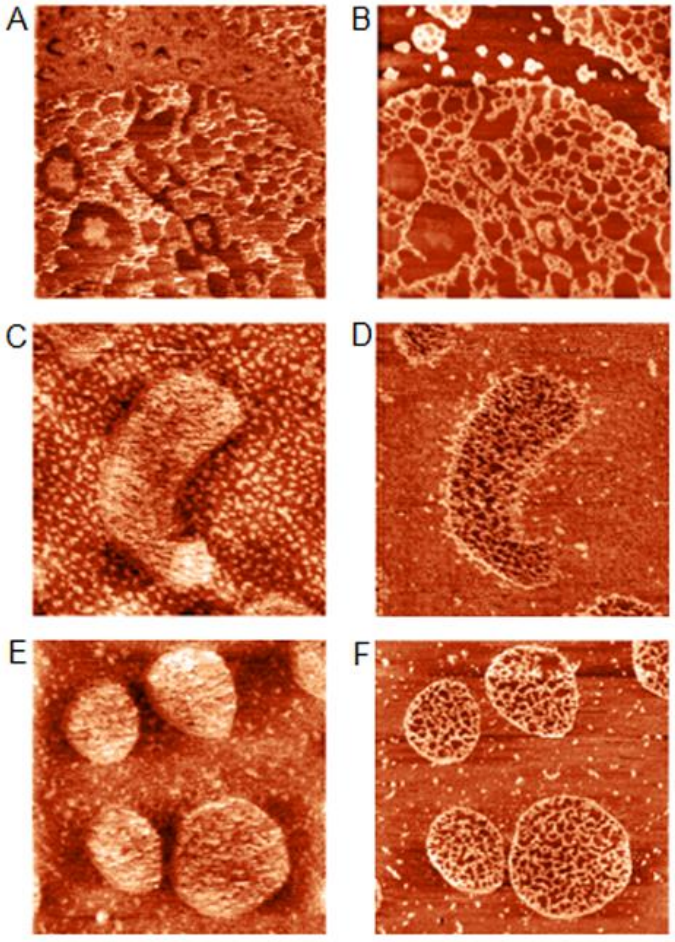

Fig.S8 Fibrous structure of the brighter domains (A and B) 0 mN m^{-1}; (C and D) 0.2 mN m^{-1}; (E and F) 1.0 mN m^{-1}

B, D and F are the phase image of A, C and E, respectively. The sizes of all images are 3 μm × 3 μm.

In Fig.S9, the fibrous structure of the brighter domains can also be acquired. From

the morphology of panel C, one can see the structure of cholesterol around the crescent domain.

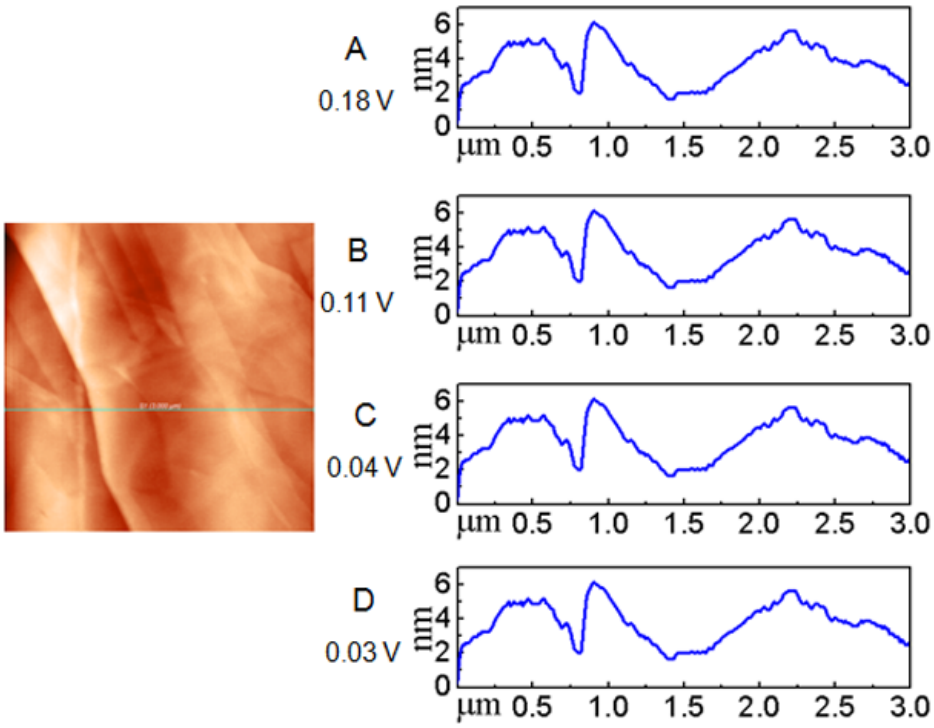

Fig.S10 Unchangeable height of highly oriented pyrolytic graphite (HOPG) with different set voltages

(A) 0.18, (B) 0.11, (C) 0.04, (D) 0.03 V